

Figure S1: Electrospray ionization mass spectrum of synthetic peptide ‘DP1’. The observed molecular ion peaks at m/z 990.05 and 660.40 correspond to the doubly charged $[M+2H]^{2+}$ and triply charged $[M+3H]^{3+}$ species, respectively, confirming the expected molecular weight (1978.48 Da) and successful peptide synthesis with correct molecular integrity.

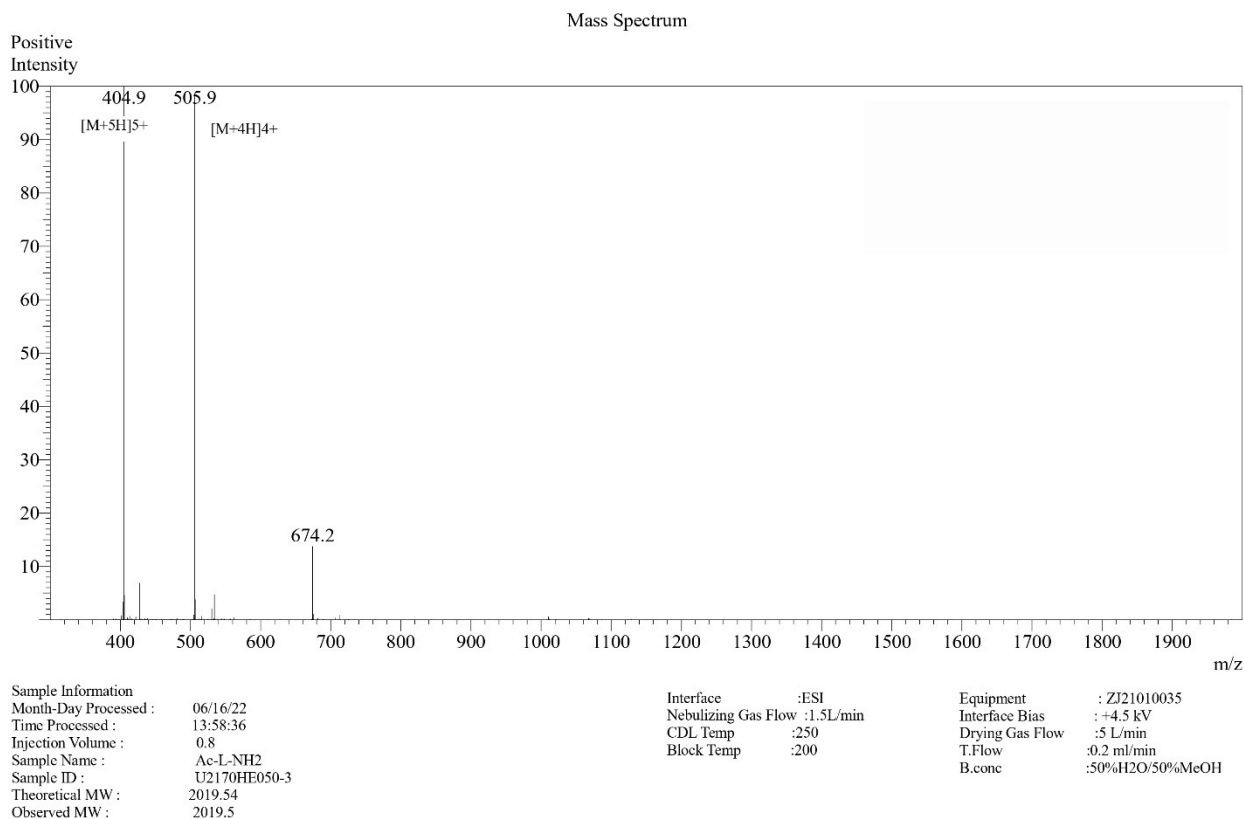


Figure S3: Electrospray ionization mass spectrum of N-terminal acetylated and C-terminal amidated peptide ‘b-DP1’. The spectrum exhibits multiple charge states, including peaks corresponding to $[M+2H]^{2+}$ and $[M+3H]^{3+}$ species, characteristic of ESI ionization of peptides. The observed molecular weight (2019.5 Da) closely matches the theoretical value (2019.54 Da), confirming successful incorporation of N-terminal acetylation and C-terminal amidation and validating the molecular integrity of the modified peptide.

Sample Name : Ac-L-NH2
 Sample ID : U2170HE050-3
 Time Processed : 6:35:28
 Month-Day-Year Processed : 06/16/2022

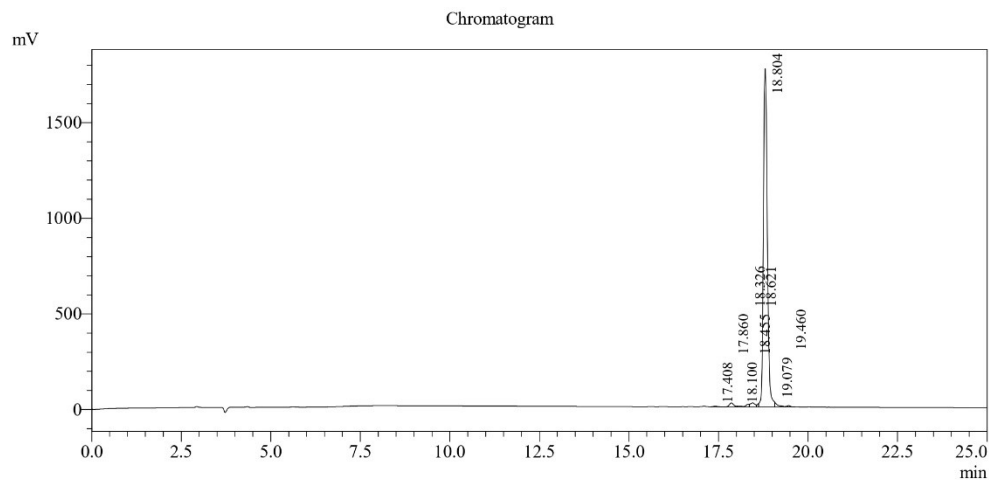
Pump A : 0.065% trifluoroacetic in 100% water (v/v)
 Pump B : 0.05% trifluoroacetic in 100% acetonitrile (v/v)
 Total Flow: 1 ml/min
 Wavelength: 220 nm

Time	Module	Command	Value
0.01	Pumps	B.Conc	5
25.00	Pumps	B.Conc	65
25.01	Pumps	B.Conc	95
27.00	Pumps	B.Conc	95
27.01	Pumps	B.Conc	5
35.00	Pumps	B.Conc	5
35.01	Controller	Stop	

<<Column Performance>>

<Detector A>

Column : Inertsil ODS-3 4.6 x 250 mm



1 Detector A Channel 1 / 220nm

Peak Table

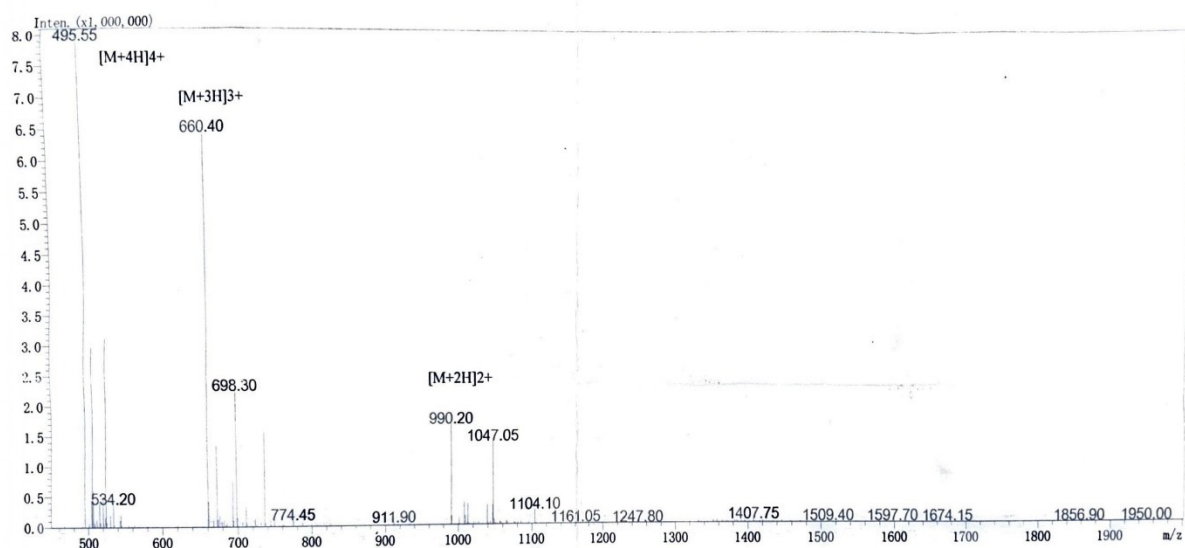
Detector A Channel 1 220nm

Peak#	Ret. Time	Area	Height	Area %
1	17.408	21887	2786	0.154
2	17.860	163764	20204	1.149
3	18.100	22452	2720	0.157
4	18.326	78919	13420	0.554
5	18.455	186745	20234	1.310
6	18.621	50856	15909	0.357
7	18.804	13564870	1767740	95.146
8	19.079	128568	23068	0.902
9	19.460	38816	6156	0.272
Total		14256877	1872237	100.000

Figure S4: Analytical RP-HPLC chromatogram of N-terminal acetylated and C-terminal amidated peptide ‘b-DP1’. The chromatogram shows a single dominant peak at a retention time of ~18.80 min with an area percentage of 95.15%, indicating high purity (>95%) of the synthesized peptide. Separation was performed on an Inertsil ODS-3 (C18) column (4.6 × 250 mm) using solvent A (0.065% TFA in water) and solvent B (0.05% TFA in acetonitrile) with a gradient of 5–65% B over 25 min at a flow rate of 1.0 mL/min, monitored at 220 nm.

MS Spectrum

Positive



Acquired by : Huang
Data Acquired : 2026/2/25
Injection Volume : 1
Sample Name : d-DP1 RK-15
Mw : 1978.48
Lot No. : P260213-YS1208188

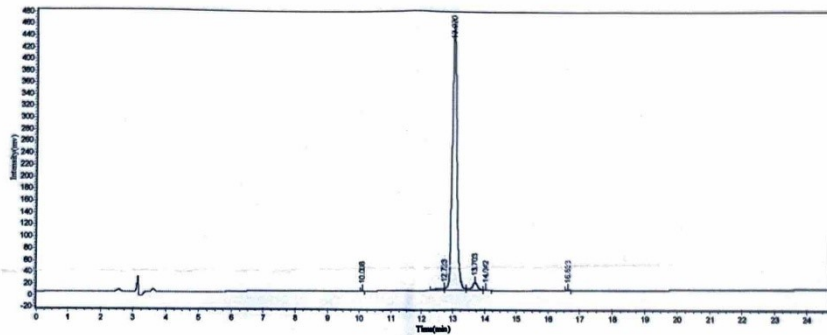
Probe : ESI Probe bias : +4.5kv
Nebulizer Gas Flow : 1.5L/min Detector : 1.2kv
CDL : -20.0v T.Flow : 0.2ml/min
CDL Temp : 250°C B.conc : 50%H₂O/50%ACN
Block Temp : 400°C

Figure S5: Electrospray ionization mass spectrum of synthetic peptide ‘D-DP1’ (all-D enantiomer). The spectrum exhibits characteristic multiply charged ion peaks corresponding to $[M+2H]^{2+}$ and $[M+3H]^{3+}$ species, consistent with the expected molecular weight of the peptide. The observed mass confirms successful synthesis and structural integrity of the D-amino acid analogue.

Structure :d-DP1 RK-15
 Lot NO :P260213-YS1208188
 Number :0200049
 Column :4.6×250mm,ChromCore 120 C18 5u
 Solvent A:0.1%TFA in 100%water
 Solvent B:0.1%TFA in 100%acetonitrile
 Gradient :

	A	B
0.1min	72%	28%
25.0min	47%	53%
25.1min	0%	100%
30.0min	stop	

 Flow rate:1.0ml/min
 Wavelength(nm):220
 Volume :10ul



Peak No.	Ret Time	Height	Area	Conc.
1	10.098	79.231	374.706	0.0078
2	12.723	2311.313	40758.047	0.8528
3	13.020	449590.500	4550510.500	95.2117
4	13.703	13360.843	170957.141	3.5770
5	14.042	1087.677	11713.761	0.2451
6	16.633	792.828	5046.391	0.1056
Total				100.00

Figure S4: Analytical RP-HPLC chromatogram of synthetic peptide ‘D-DP1’ showing a single dominant peak, confirming a purity of >95%. Chromatographic separation was performed under conditions identical to those used for DP1, employing a ChromCore 120 C18 column with a gradient of 5–100% acetonitrile (0.1% TFA) over 25 min at a flow rate of 1.0 mL/min and detection at 220 nm.

All characterization data collectively confirm that the synthesized peptides possess high purity (>95%) and correct molecular mass, ensuring that the observed biological activities are attributable solely to the peptides.

Table S1. Comparative resistance development profiles of the peptides with clinically relevant antibiotics against MRSA and *Pseudomonas aeruginosa* under serial passaging conditions. Data for antibiotics are compiled from published peer-reviewed studies employing *in vitro* serial passaging and the peptide data are from the present study.

S. No.	Antibacterial agent	Class & mechanism of action	Target pathogen	Passaging duration	Reported fold-MIC increase	Primary resistance mechanism	Reference
1	Ciprofloxacin	Fluoroquinolone; DNA gyrase & topoisomerase IV inhibition	MRSA	<i>In vitro</i> pharmacodynamic simulation (5 days, clinical dosing)	8–32×	grlA and gyrA point mutations; NorA efflux upregulation	1
2	Ofloxacin	Fluoroquinolone; DNA gyrase inhibition	<i>S. aureus</i> ATCC 29213	~25 days serial passage (sub-MIC)	>256× (maximum tested)	gyrA / grlA mutations	2
3	Levofloxacin	Fluoroquinolone; DNA gyrase inhibition	MRSA	<i>In vitro</i> pharmacodynamic modeling (low-dose regimens)	Up to 16×	grlA, gyrA, grlB sequential mutations	3
4	Meropenem	Carbapenem; PBP inhibition, cell-wall biosynthesis	<i>P. aeruginosa</i> PA14	11–13 passages	Up to ~64× (from ≤0.25 to 16 µg/mL)	oprD inactivation + mexR mutation leading to MexAB-OprM efflux upregulation	4
5	Gentamicin	Aminoglycoside; 30S ribosomal subunit inhibition	<i>P. aeruginosa</i> (clinical evolution)	Sequential clinical isolates under therapy	≥4× (clonal pair MIC escalation)	MexXY-OprM efflux upregulation; aminoglycoside-modifying enzymes	5
6	Tobramycin	Aminoglycoside; 30S ribosomal subunit inhibition	<i>P. aeruginosa</i>	Serial <i>in vitro</i> evolution	≥8×	MexXY-OprM efflux; enzymatic inactivation	6
7	Vancomycin	Glycopeptide; D-Ala-D-Ala binding, leading to cell-wall inhibition	MRSA	Stepwise <i>in vitro</i> selection with increasing concentrations	From 1 to ≥32 µg/mL (≥32×; VISA/VRSA phenotype)	Cell-wall thickening; accumulated mutations in walK, graR, rpoB, vraS	7, 8
8	Vancomycin	Glycopeptide; D-Ala-D-Ala binding,	MRSA (clinical;	<i>In vivo</i> evolution during prolonged	8× (From 1 to 8 µg/mL;	Stepwise regulatory mutations; reduced	9

S. No.	Antibacterial agent	Class & mechanism of action	Target pathogen	Passaging duration	Reported fold-MIC increase	Primary resistance mechanism	Reference
		leading to cell-wall inhibition	serial isolates from single patient)	therapy	hVISA → VISA progression)	autolysis	
9	Colistin	Polymyxin; LPS / lipid A disruption	<i>P. aeruginosa</i> (XDR clinical isolates)	Morbidostat continuous culture	10× within 10 days; 100× within 20 days	pmrAB mutations + lpxC, pmrE, migA mutations leading to L-Ara4N lipid A modification	10
10	Ciprofloxacin (<i>in vivo</i>)	Fluoroquinolone; DNA gyrase inhibition	MRSA (hospital clinical surveillance)	3–12 months of hospital ciprofloxacin use	>100× (MIC ₉₀ rose from susceptible baseline to 64 µg/mL)	gyrA / grlA mutations; clonal resistance spread	11
11	DP1	Synthetic AMP; membrane-disruptive	MRSA & <i>P. aeruginosa</i>	10 serial passages (sub-MIC exposure)	No change (1×)	None detected	This study
12	b-DP1	Synthetic AMP; membrane-disruptive	MRSA & <i>P. aeruginosa</i>	10 serial passages (sub-MIC exposure)	No change (1×)	None detected	This study
13	D-DP1	Synthetic AMP; membrane-disruptive (all-D enantiomer)	MRSA & <i>P. aeruginosa</i>	10 serial passages (sub-MIC exposure)	No change (1×)	None detected	This study

Notes: MIC, minimum inhibitory concentration; MRSA, methicillin-resistant *Staphylococcus aureus*; VISA, vancomycin-intermediate *S. aureus*; VRSA, vancomycin-resistant *S. aureus*; XDR, extensively drug-resistant; LPS, lipopolysaccharide; AMP, antimicrobial peptide; PBP, penicillin-binding protein

References

1. J. J. Campion, P. J. McNamara and M. E. Evans, *Antimicrobial Agents and Chemotherapy*, 2004, 48, 4733–4744.

2. L. L. Ling, T. Schneider, A. J. Peoples, A. L. Spoering, I. Engels, B. P. Conlon, A. Mueller, T. F. Schäberle, D. E. Hughes, S. Epstein, M. Jones, L. Lazarides, V. A. Steadman, D. R. Cohen, C. R. Felix, K. A. Fetterman, W. P. Millett, A. G. Nitti, A. M. Zullo, C. Chen and K. Lewis, *Nature*, 2015, 517, 455–459.
3. J. J. Champion, P. Chung, P. J. McNamara, W. B. Titlow and M. E. Evans, *Antimicrobial Agents and Chemotherapy*, 2005, 49, 2189–2199.
4. J. Feng, Y. Bian, C. Xu, Z. Cheng, Y. Jin, S. Jin and W. Wu, *Microorganisms*, 2025, 13, 1672.
5. M. Riou, S. Carbonnelle, L. Avrain, N. Mesaros, J.-P. Pirnay, F. Bilocq, D. De Vos, A. Simon, D. Piérard, F. Jacobs, A. Dediste, P. M. Tulkens, F. Van Bambeke and Y. Glupczynski, *International Journal of Antimicrobial Agents*, 2010, 36, 513–522.
6. D. Hocquet, P. Nordmann, F. E. Garch, L. Cabanne and P. Plésiat, *Antimicrobial Agents and Chemotherapy*, 2006, 50, 1347–1351.
7. K. Ishii, F. Tabuchi, M. Matsuo, K. Tatsuno, T. Sato, M. Okazaki, H. Hamamoto, Y. Matsumoto, C. Kaito, T. Aoyagi, K. Hiramatsu, M. Kaku, K. Moriya and K. Sekimizu, *Scientific Reports*, 2015, 5, 17092.
8. B. P. Howden, C. R. E. McEvoy, D. L. Allen, K. Chua, W. Gao, P. F. Harrison, J. Bell, G. Coombs, V. Bennett-Wood, J. L. Porter, R. Robins-Browne, J. K. Davies, T. Seemann and T. P. Stinear, *PLOS Pathogens*, 2011, 7, e1002359.
9. K. Hiramatsu, Y. Kayayama, M. Matsuo, Y. Aiba, M. Saito, T. Hishinuma and A. Iwamoto, *Journal of Global Antimicrobial Resistance*, 2014, 2, 213–224.
10. B. Döbelmann, M. Willmann, M. Steglich, B. Bunk, U. Nübel, S. Peter and R. A. Neher, *Antimicrobial Agents and Chemotherapy*, 2017, 61, e00043–00017.
11. L. R. Peterson, J. N. Quick, B. Jensen, S. Homann, S. Johnson, J. Tenquist, C. Shanholtzer, R. A. Petzel, L. Sinn and D. N. Gerding, *Archives of Internal Medicine*, 1990, 150, 2151–2155.